

Mapping the catalytic pocket of phospholipases A₂ and C using a novel set of phosphatidylcholines

Julio J. CAMELO*, Jorge FLORÍN-CHRISTENSEN†, Mónica FLORÍN-CHRISTENSEN† and José M. DELFINO*¹

*Department of Biological Chemistry and Institute of Biochemistry and Biophysics (IQUIFIB), School of Pharmacy and Biochemistry, University of Buenos Aires, Junín 956, 1113 Buenos Aires, Argentina, and †College of Veterinary Medicine, Washington State University, Pullman, WA 99164-7010, U.S.A.

A set of radioiodinatable phosphatidylcholines (PCs) derivatized with the Bolton–Hunter reagent (BHPCs) was synthesized to probe the substrate recognition and activity of phospholipases. A common feature of this series is the presence of a bulky 4-hydroxyphenyl group at the end of the fatty acyl chain attached to position *sn*-2. The distance between the end group and the glycerol backbone was varied by changing the length of the intervening fatty acyl chain (3–25 atoms). Except for the shortest, this chain includes at least one amide linkage. The usefulness of this series of substrates as a molecular ruler was tested by measuring the hydrolytic activities of *Naja naja naja* phospholipase A₂ (PLA₂) and *Bacillus cereus* phospholipase C (PLC) in Triton X-100 micelles. The activity of PLA₂ proved to be highly dependent on the length of the fatty acyl chain linker, the shorter compounds (3–10 atoms) being very poor substrates. In contrast, the PLC activity profile exhibited much less discrimination. In both cases, PCs with 16–21 atom chains at position *sn*-2 yielded

optimal activity. We interpret these findings in terms of fatty acyl chain length-related steric hindrance caused by the terminal aromatic group, affecting the activity of PLA₂ and, to a smaller extent, that of PLC. This notion agrees with the more extended recognition of aliphatic chains inside the narrow channel leading to the catalytic site in the former case. Molecular models of these substrates bound to PLA₂ were built on the basis of the crystallographic structure of *Naja naja atra* PLA₂ complexed with a phospholipid analogue. Docking of these substrates necessarily requires the intrusion of the bulky 4-hydroxyphenyl group inside the binding pocket and also the failure of the amide group to form hydrogen bonds inside the hydrophobic substrate channel.

Key words: molecular docking, phospholipid synthesis, radioiodinatable phosphatidylcholines, substrate recognition, water/lipid interface.

INTRODUCTION

There is mounting evidence that different phospholipases have key roles in signal transduction [1–6]. Understanding the mechanisms underlying the regulation of these enzymes is a challenging issue in this field. This requires the analysis of the molecular traits controlling catalysis, including the architecture and function of the catalytic site and the hydrophobic pocket leading to it. A hindrance at this level can be envisaged as a possible site for regulation because it would restrict the access of the phospholipid substrate to the catalytic site. It is therefore important to test possible structural changes in this hydrophobic pocket occurring on the operation of regulatory mechanisms. For instance, with cytosolic phospholipase A₂ (PLA₂), Ca²⁺ binding to an N-terminal C2 domain is accepted as an important regulatory event. In addition, phosphorylation by mitogen-activated protein kinase is another mechanism controlling PLA₂ activity [7]. Both of these effects might alter the structure of the hydrophobic pocket. These hypotheses can be tested with the novel series of phospholipid substrates presented here, which sense restrictions to substrate access to the catalytic site.

In their natural milieu, both PLA₂ and phospholipase C (PLC) work at membrane/water interfaces; catalytic activity has been shown to increase markedly when these enzymes are exposed to

aggregated substrates, i.e. above the critical micelle concentration [8,9]. Several studies have defined the structural requirements for phospholipids to become substrates of phospholipases [9–11]. For optimal PLA₂ activity, a minimal fatty acyl chain of seven carbon atoms is needed; no steric hindrance should exist near the glycerol backbone. Besides, no impediment should preclude the upward motion of the substrate from the lipid phase into the catalytic site, e.g. by anchoring the tail of the fatty acid to a polymeric support [12,13]. More generally, any structural feature of the substrate that restricts the vertical movement of the molecule markedly affects enzymic activity. In contrast, PLC is less stringent than PLA₂ in its substrate requirements, the chain length dependence is not so important, and a constraint on the vertical motion of the substrate does not seem to affect enzymic activity negatively [12,13]. In the light of the structures of several phospholipases, crystallized in their isolated forms or in complexes with substrate analogues [14–17], the existence of hydrophobic channels leading to the catalytic sites was proposed. This view supports the notion that, for catalysis by PLA₂ to occur, a deep burrowing of the substrate into the protein should take place [18]. In contrast, PLC exhibits a shallow cleft for docking the phospholipid substrate.

The use of molecular probes to measure distances in biological systems is well established. Examples of this are the ruler type of

Abbreviations used: BH, Bolton–Hunter [3-(4-hydroxyphenyl)propionic acid]; BHPC(s), phosphatidylcholine(s) derivatized with the Bolton–Hunter reagent; BHR, Bolton–Hunter reagent [3-(4-hydroxyphenyl)propionic acid, succinimidyl ester]; tBOC, t-butoxycarbonyl; DCC, 1,3-dicyclohexylcarbodiimide; DMAP, 4-dimethylaminopyridine; PC, phosphatidylcholine; PDB, Brookhaven protein data bank; PLA₂, phospholipase A₂; PLC, phospholipase C; THF, tetrahydrofuran.

¹ To whom correspondence should be addressed (e-mail rtdelfin@criba.edu.ar).

fluorophores [19] and spin-labelled probes [20] for studying the hydrophobic membrane domain at various depths. To gain further insight into substrate recognition by these phospholipases, we describe here the design and synthesis of a novel set of phosphatidylcholines (PCs) endowed with fatty acids of variable length esterifying the *sn*-2 position of the glycerol moiety. To preserve recognition by the enzymes at the critical polar head group, no modifications were allowed therein. However, a distinctive feature of this family consists of the presence of a distal 4-hydroxyphenyl group attached to the end of the fatty acyl chain. The rationale behind this design was to provide a bulky end to the fatty acid chain, as a source of steric hindrance. In addition, this functional group can be readily radioiodinated through a usual oxidative procedure, thus allowing an easy quantification of the reaction products. Using these novel compounds we analyse here features of substrate recognition by *Naja naja naja* PLA₂ and *Bacillus cereus* PLC. In addition, we present computer modelling studies on the docking of each substrate to PLA₂, accounting for the differential behaviour of this enzyme towards each PC analogue. This study therefore provides a new method for the functional analysis of PLA₂ catalysis. More generally, this work introduces a family of PCs useful by themselves or as a source of derivatives (e.g. *sn*-1,2-diacylglycerol, phosphatidic acid or fatty acid) for probing the size and nature of the pocket in lipid-binding proteins.

MATERIALS AND METHODS

Materials

N. naja naja PLA₂, *B. cereus* PLC, egg yolk L- α -lysoPC (type I), 4-dimethylaminopyridine (DMAP), 3-(4-hydroxyphenyl)propionic acid, Bolton–Hunter reagent [BHR; 3-(4-hydroxyphenyl)propionic acid, succinimidyl ester], 4-aminobutanoic acid, 6-aminohexanoic acid, 8-amino-octanoic acid, 12-aminododecanoic acid, Hepes, CaCl₂ and Triton X-100 were purchased from Sigma Chemical Co. (St Louis, MO, U.S.A.). Zinc dust, ZnCl₂, *N*-hydroxysuccinimide and 1,3-dicyclohexylcarbodiimide (DCC) were purchased from Aldrich Chemical Co. (Milwaukee, WI, U.S.A.). Trifluoroacetic acid was supplied by Riedel de Haën (Seelze-Hannover, Germany). Na¹²⁵I (15–17 Ci/mg) was obtained from New England Nuclear (Boston, MA, U.S.A.). Chloroform was refluxed from P₂O₅, distilled before use (b.p. 59–60 °C) and stored in a brown glass bottle. Tetrahydrofuran (THF) was refluxed from CaH₂ and distilled before use. All other organic solvents were of reagent-grade quality, obtained from E. Merck (Darmstadt, Germany) and used without further purification.

General procedures

¹H-NMR (w/v) spectra were recorded on a Bruker MSL 300 spectrometer, UV-visible spectra were determined with a Jasco 7850 spectrophotometer and radioactivity from ¹²⁵I was measured with a Wallac 1272 Clinigamma scintillation counter. TLC was routinely performed on 5.0 cm × 1.6 cm plates of silica gel 60 F₂₅₄ (E. Merck). Solvent systems employed were as follows: solvent 1, chloroform/methanol/water/acetic acid (65:25:4:1, by vol.); solvent 2, light petroleum (boiling range 30–60 °C)/diethyl ether/acetic acid (70:30:1, by vol.); solvent 3, chloroform/methanol (10:1, v/v); solvent 4, chloroform/methanol/water/acetic acid (65:25:1:0.5, by vol.). Spots on TLC plates were detected by fluorescence quenching under illumination with a UV source (254 nm) and/or staining with the following reagents: Molybdenum Blue (Sigma), iodine vapour or ninhydrin (0.2% in acetone). TLC plates containing ¹²⁵I-labelled

products were covered with Kodak XAR-5 film for autoradiography, and the film was exposed in the dark.

Synthesis and characterization of compounds

3-(4-Acetoxyphenyl)propionic acid (**9**)

Compound **8** {Bolton–Hunter [BH, 3-(4-hydroxyphenyl)propionic acid] 400 mg, 2.4 mmol, UV positive spot of *R_F* 0.22 by TLC developed in solvent 3} (see Scheme 1) and acetic anhydride (250 mg, 3.37 mmol) were dissolved in anhydrous chloroform (10 ml) and the mixture was cooled to 0 °C. The reaction was catalysed by the addition of a drop of concentrated (18 M) H₂SO₄. After 5 h, water (50 μ l, 2.77 mmol) was added to the reaction mixture to quench the remaining anhydride. After incubation for a further 40 min, the solution was concentrated to dryness under reduced pressure and the solid residue was dissolved in chloroform. Product **9** was purified by silica-gel column chromatography, with chloroform as the solvent. Compound **9** (397 mg, 1.9 mmol; 79% yield) was a single spot by TLC (UV-positive spot of *R_F* 0.46 in solvent 3).

Anhydride of 3-(4-acetoxyphenyl)propionic acid

The procedure followed was similar to that described by Delfino et al. [13] for the synthesis of anhydrides of *N*-tBOC-amino acids (in which tBOC stands for t-butoxycarbonyl): **9** (92 mg, 0.44 mmol) was dissolved in freshly distilled dry chloroform (2 ml) and the solution was cooled in an ice bath. To this stirred solution a recently prepared solution of DCC (45 mg, 0.22 mmol) in a minimal volume of dry chloroform was added dropwise. The reaction flask was gassed with nitrogen and capped tightly. After 5 min at 0 °C, the reaction mixture was left to warm to 25 °C. The appearance of a white precipitate of 1,3-dicyclohexylurea was evident after 10–15 min. After 2 h the precipitate was removed by filtration through glass wool; the solution was used immediately in the coupling reaction to egg yolk lysoPC. TLC analysis of this solution (in solvent 3) revealed a major spot that migrated close to the solvent front.

1-Fatty acyl-2-[3-(4-acetoxyphenyl)propionyl] PC (Ac-BH-C0PC, **10**)

The coupling method followed here was similar to that described by Gupta et al. [21], with minor modifications. LysoPC was dissolved in dry chloroform, the solvent was evaporated under a nitrogen stream and traces of water or alcohols were removed azeotropically by washing the sample three times with dry toluene and evaporating this solvent under high vacuum. LysoPC (25 mg, approx. 0.055 mmol) was finally dissolved in dry chloroform. To this solution was then added DMAP (10 mg, 0.082 mmol). At this point the mixture was cooled in an ice-bath before the solution containing the previously prepared anhydride (0.22 mmol, approx. 4-fold excess over lysoPC) was added dropwise with constant stirring. After 5–6 h at 25 °C, the reaction was essentially complete, as revealed by the disappearance of lysoPC (*R_F* 0.1 by TLC in solvent 1) and the appearance of product **10** (*R_F* 0.43). At the end this compound was purified from the reaction mixture by silica-gel column chromatography: excess anhydride of **9**, compound **9** itself and DMAP were eluted first with solvent 3; product **10** was then eluted with solvent 4 (more than 80% yield). ¹H-NMR (C²HCl₃, 300 MHz): the spectrum of **10** showed characteristic broadening typical of phospholipids, δ 0.87 (t, 3H), 1.26 (m, 24–28H), 1.56 (m, 2H), 2.27 (m, 5H), 2.67 (t, 2H), 2.92 (t, 2H), 3.29 (s, 9H), 3.88 (broad, 2H), 4.16 (broad, 2H), 4.31–4.50 (broad and complex, 4H), 5.25 (broad, 1H), 6.97 (d, 2H), 7.22 (d, 2H). TLC analysis of **10**

showed a single spot (R_f 0.43 in solvent 1) after staining with Molybdenum Blue or iodine vapour.

1-Fatty acyl-2-[3-(4-hydroxyphenyl)-propionyl] PC (BH-COPC, **1**) (see Figure 1)

Selective removal of the acetyl group in compound **10** was achieved by following a technique appropriate for cleavage of aryl esters [22]. Typically, **10** (20 mg, approx. 0.032 mmol) was dissolved in dry methanol (0.5 ml). To this solution, activated Zn dust (2.5 mg, 0.038 mmol) was added with constant stirring. After 1 h at 25 °C, the reaction mixture was filtered through Celite to remove solid material, the solvent was then evaporated under reduced pressure and product **1** was purified by silica-gel column chromatography with solvent 4 (84% yield). $^1\text{H-NMR}$ (C^2HCl_3 , 300 MHz): the spectrum of **1** showed characteristic broadening typical of phospholipids, δ 0.81 (t, 3H), 1.22 (m, 24–28H), 1.52 (m, 2H), 2.21 (t, 2H), 2.55 (t, 2H), 2.80 (t, 2H), 3.02 (s, 9H), 3.35 (m, 2H), 3.87 (broad, 2H), 3.95–4.10 (complex, 3H), 4.25 (complex, 1H), 5.08 (m, 1H), 6.65 (d, 2H), 6.95 (d, 2H). TLC analysis of **1** revealed a single spot (R_f 0.26 in solvent 1) after staining with Molybdenum Blue or iodine vapour.

4-(N-tBOC)aminobutanoic acid (**11**), 6-(N-tBOC)aminohexanoic acid (**12**), 8-(N-tBOC)amino-octanoic acid (**13**) and 12-(N-tBOC)aminododecanoic acid (**14**) (see Scheme 2)

Protection of the amino group of the ω -amino acids was performed by following a common general technique [13]. Each ω -amino acid (1.13–2.37 g, 11 mmol; R_f 0.0 by TLC in solvent 3, spots stained purple with ninhydrin) was dissolved in THF/ aqueous NaOH [100 ml, 2:1 (v/v); 0.5 g NaOH, 12.5 mmol]. DMAP (1.4 g, 11.5 mmol) was then added and the mixture was cooled to 0 °C. The reaction was started by the dropwise addition to this stirred solution of di-*t*-butyl pyrocarbonate (2.8 g, 12.8 mmol) dissolved in THF. After 5 min at 0 °C, the reaction mixture was kept at 25 °C for 16 h with constant stirring. At the end, the solvent was evaporated under reduced pressure and diethyl ether was added to the remaining aqueous phase. After acidification to pH 1 with concentrated HCl, the aqueous layer was quickly extracted three times with diethyl ether. The combined extracts were washed first with dilute aqueous HCl and secondly with water. Finally, the combined extract was dried with MgSO_4 and filtered; the solvent was evaporated under reduced pressure. Traces of solvents were further removed under high vacuum. The white remaining powder was essentially pure product (**11–14**, 80% typical yields). When necessary, further purification of each product was accomplished by silica-gel column chromatography in solvent 3. Analysis of each product by TLC developed in solvent 3 showed a single spot (all compounds showed an R_f of approx. 0.5) after staining with iodine vapour. These products did not react with ninhydrin.

Anhydrides of N-tBOC- ω -amino acids

Anhydrides of compounds **11–14** were synthesized by following the same technique as that described above for the synthesis of the anhydride of compound **9**.

1-Fatty acyl-2-[4-(N-tBOC)aminobutanoyl] PC (**15**, N-tBOC-C4PC), 1-fatty acyl-2-[6-(N-tBOC)aminohexanoyl] PC (**16**, N-tBOC-C6PC), 1-fatty acyl-2-[8-(N-tBOC)amino-octanoyl] PC (**17**, N-tBOC-C8PC) and 1-fatty acyl-2-[12-(N-tBOC)aminododecanoyl] PC (**18**, N-tBOC-C12PC)

Acylation of lysoPC with the corresponding anhydrides of the ω -(N-tBOC)amino acids was accomplished by following a similar

protocol to that described above for the synthesis and purification of compound **10**. The TLC analysis of each product in solvent 1 revealed a single spot after staining with Molybdenum Blue or exposure to iodine vapour. Typical yields ranged between 70% and 85%. To prevent excessive line broadening of $^1\text{H-NMR}$ signals, for some of these compounds a small amount of $\text{C}^2\text{H}_3\text{O}^2\text{H}$ was added to C^2HCl_3 . **15**: TLC: R_f 0.45. $^1\text{H-NMR}$ [$\text{C}^2\text{HCl}_3/\text{C}^2\text{H}_3\text{O}^2\text{H}$, 10:1 (v/v), 300 MHz]: δ 0.65 (t, 3H), 1.07 (m, 24–28H), 1.20 (s, 9H), 1.35 (m, 2H), 1.55 (m, 2H), 2.12 (overlapping triplets, 4H), 2.85 (m, 2H), 2.97 (s, 9H), 3.46 (t, 2H), 3.66 (m, 2H), 3.92 (m, 1H), 3.98 (broad, 2H), 4.17 (dd, 1H), 4.99 (m, 1H). **16**: TLC: R_f 0.46. $^1\text{H-NMR}$ (C^2HCl_3 , 300 MHz): δ 0.88 (t, 3H), 1.24 (m, 26–30H), 1.42 (s, 9H), 1.60 (m, 6H), 2.31 (overlapping triplets, 4H), 3.10 (m, 2H), 3.32 (s, 9H), 3.68 (broad, 2H), 3.95 (broad, 2H), 4.11 (broad, 1H), 4.32 (broad and complex, 3H), 4.83 (broad, 1H), 5.20 (m, 1H). **17**: TLC: R_f 0.46. $^1\text{H-NMR}$ [$\text{C}^2\text{HCl}_3/\text{C}^2\text{H}_3\text{O}^2\text{H}$, 10:1 (v/v), 300 MHz]: δ 0.75 (t, 3H), 1.15 (m, 30–34H), 1.42 (s, 9H), 1.49 (m, 6H), 2.19 (overlapping triplets, 4H), 2.95 (m, 2H), 3.12 (s, 9H), 3.48 (broad, 2H), 3.90 (broad, 2H), 4.01 (m, 1H), 4.12 (complex, 2H), 4.29 (dd, 1H), 5.10 (m, 1H). **18**: TLC: R_f 0.47. $^1\text{H-NMR}$ (C^2HCl_3 , 300 MHz): δ 0.86 (t, 3H), 1.27 (m, 38–42H), 1.43 (s, 9H), 1.58 (m, 6H), 2.28 (overlapping triplets, 4H), 3.07 (m, 2H), 3.28 (s, 9H), 3.77 (broad, 2H), 3.94 (t, 2H), 4.11 (dd, 1H), 4.33 (broad and complex, 2H), 4.52 (broad, 1H), 5.17 (m, 1H).

4-(N-tBOC)aminobutanoic acid, succinimidyl ester (**19**) and 8-(N-tBOC)amino-octanoic acid, succinimidyl ester (**20**) (see Scheme 3)

These reagents useful for adding spacer arms were prepared as follows. Compound **11** or **13** (6.1 mg or 7.8 mg, 0.03 mmol) and *N*-hydroxysuccinimide (3.8 mg, 0.033 mmol) were dissolved in dry THF (1–2 ml) and cooled in an ice bath. A solution of DCC (6.8 mg, 0.033 mmol) in a minimal volume of THF was added dropwise to this stirred solution. A heavy white precipitate of 1,3-dicyclohexylurea appeared after 10–15 min. After 5 h the reaction mixture was filtered to remove this precipitate, the solvent was evaporated under reduced pressure and the solid residue was resuspended in a minimal volume of dry chloroform. Analysis of each product by TLC developed in solvent 3 showed a single spot (both **19** and **20** showed R_f values of approx. 0.95). These compounds were not characterized further and were used immediately in the coupling reaction to **26**.

1-fatty acyl-2-[12-[4-(N-tBOC)aminobutanoyl]-aminododecanoyl] PC (**21**, N-tBOC-C16PC) and 1-fatty acyl-2-[12-[8-(N-tBOC)amino-octanoyl]-aminododecanoyl] PC (**22**, N-tBOC-C20PC)

Each succinimidyl ester (**19** or **20**, 0.03 mmol) suspended in dry chloroform was added to a stirred solution of **26** (17.7 mg, approx. 0.025 mmol) and DMAP (3.4 mg, 0.028 mmol) in chloroform/methanol (5:1, v/v; 1 ml). After 2 h at 25 °C, the solvent was evaporated under reduced pressure and the product was purified by silica-gel column chromatography as described above (80–85% yield). The TLC behaviour of **21** and **22** in solvent 1 was similar to that of **18**. **21**: TLC: R_f 0.47. $^1\text{H-NMR}$ [$\text{C}^2\text{HCl}_3/\text{C}^2\text{H}_3\text{O}^2\text{H}$, 10:1 (v/v), 300 MHz]: δ 0.67 (t, 3H), 1.07 (m, 38–42H), 1.21 (s, 9H), 1.38 (m, 6H), 1.51 (m, 2H), 1.94 (t, 2H), 2.09 (overlapping triplets, 4H), 2.84 (m, 2H), 2.94 (m, 2H), 3.00 (s, 9H), 3.49 (broad, 2H), 3.78 (m, 2H), 3.92 (m, 1H), 4.03 (m, 2H), 4.18 (dd, 1H), 5.00 (m, 1H). **22**: TLC: R_f 0.48. $^1\text{H-NMR}$ (C^2HCl_3 , 300 MHz): δ 0.89 (t, 3H), 1.27 (m, 46–50H), 1.46 (s, 9H), 1.58 (m, 6H), 2.14 (t, 2H), 2.30 (overlapping triplets, 4H), 3.07 (m, 2H), 3.20 (m, 2H), 3.32 (s, 9H), 3.78 (broad, 2H), 3.97 (m, 2H), 4.00–4.40 (broad and complex, 4H), 4.58 (broad, 1H), 5.20 (m, 1H), 5.71 (broad, 1H).

1-Fatty acyl-2-(4-aminobutanoyl) PC (**23**, C4PC), 1-fatty acyl-2-(6-aminohexanoyl) PC (**24**, C6PC), 1-fatty acyl-2-(8-amino-octanoyl) PC (**25**, C8PC), 1-fatty acyl-2-(12-aminododecanoyl) PC (**26**, C12PC), 1-fatty acyl-2-[12-(4-aminobutanoyl)-aminododecanoyl] PC (**27**, C16PC) and 1-fatty acyl-2-[12-(8-amino-octanoyl)-aminododecanoyl] PC (**28**, C20PC)

Deprotection of the terminal amino group was achieved with trifluoroacetic acid [13]. Compounds **15–18** or **21–22** (approx. 0.031 mmol) were dissolved in chloroform (2 ml) and the solution was cooled to 0 °C in an ice bath. To this stirred solution, methanol (0.15 ml) and trifluoroacetic acid (2 ml) were added dropwise. The flask was flushed with nitrogen and capped tightly. After 40 min at 0 °C, the solvents were evaporated under a stream of nitrogen at 0 °C. Traces of trifluoroacetic acid were eliminated by repeated washings with chloroform/methanol (1 : 1, v/v) and evaporation under high vacuum. Purification of each product was achieved by silica-gel column chromatography, employing firstly solvent 3 and then solvent 1. Yields of pure products (**23–28**) ranged between 70 % and 75 %. TLC analysis of each compound in solvent 1 revealed a single spot (R_f approx. 0.17) after staining with Molybdenum Blue, or a single purple spot after staining with ninhydrin. To prevent excessive line broadening of $^1\text{H-NMR}$ signals, for some of these compounds a small amount of $\text{C}^2\text{H}_3\text{O}^2\text{H}$ was added to C^2HCl_3 . **23**: $^1\text{H-NMR}$ [$\text{C}^2\text{HCl}_3/\text{C}^2\text{H}_3\text{O}^2\text{H}$, 10 : 1 (v/v), 300 MHz]: δ 0.88 (t, 3H), 1.25 (m, 24–28H), 1.59 (m, 2H), 2.02 (m, 4H), 2.31 (t, 2H), 2.99 (m, 2H), 3.22 (s, 9H), 3.64 (broad, 2H), 3.94 (broad, 2H), 4.00–4.33 (broad and complex, 4H), 5.21 (m, 1H). **24**: $^1\text{H-NMR}$ [$\text{C}^2\text{HCl}_3/\text{C}^2\text{H}_3\text{O}^2\text{H}$, 10 : 1 (v/v), 300 MHz]: δ 0.87 (t, 3H), 1.25 (m, 26–30H), 1.45 (m, 2H), 1.64 (m, 4H), 2.34 (overlapping triplets, 4H), 2.89 (m, 2H), 3.22 (s, 9H), 3.64 (broad, 2H), 3.95 (broad, 2H), 4.00–4.32 (broad and complex, 4H), 5.26 (m, 1H). **25**: $^1\text{H-NMR}$ [$\text{C}^2\text{HCl}_3/\text{C}^2\text{H}_3\text{O}^2\text{H}$, 10 : 1 (v/v), 300 MHz]: δ 0.88 (t, 3H), 1.25 (m, 30–34H), 1.58 (m, 6H), 2.31 (overlapping triplets, 4H), 2.89 (m, 2H), 3.38 (s, 9H), 3.87 (broad, 2H), 3.96 (broad, 2H), 4.14–4.33 (broad and complex, 4H), 5.25 (m, 1H). **26**: $^1\text{H-NMR}$ [$\text{C}^2\text{HCl}_3/\text{C}^2\text{H}_3\text{O}^2\text{H}$, 10 : 1 (v/v), 300 MHz]: δ 0.86 (t, 3H), 1.27 (m, 38–42H), 1.43 (s, 9H), 1.58 (m, 6H), 2.25 and 2.29 (overlapping triplets, 4H), 2.82 (m, 2H), 3.27 (s, 9H), 3.73 (broad, 2H), 3.90 (broad, 2H), 4.01–4.44 (broad and complex, 4H), 5.18 (m, 1H). **27**: $^1\text{H-NMR}$ (C^2HCl_3 , 300 MHz): δ 0.88 (t, 3H), 1.24 (m, 38–42H), 1.53 (m, 6H), 2.01 (m, 2H), 2.31 (broad, 6H), 2.95 (m, 2H), 3.16 (broad, 2H), 3.37 (s, 9H), 3.85 (broad, 2H), 3.94 (m, 2H), 4.12–4.35 (broad and complex, 4H), 5.20 (m, 1H). **28**: $^1\text{H-NMR}$ (C^2HCl_3 , 300 MHz): δ 0.87 (t, 3H), 1.25 (m, 46–50H), 1.46 (m, 2H), 1.54 (m, 6H), 2.15 (t, 2H), 2.28 (overlapping triplets, 4H), 2.85 (m, 2H), 3.12 (m, 2H), 3.30 (s, 9H), 3.60 (broad, 2H), 3.96 (m, 2H), 4.11–4.21 (broad and complex, 3H), 4.35 (dd, 1H), 5.21 (m, 1H).

1-Fatty acyl-2-{4-[3-(4-hydroxyphenyl)-propionyl]-aminobutanoyl} PC (**2**, BH-C4PC), 1-fatty acyl-2-{6-[3-(4-hydroxyphenyl)-propionyl]-aminohexanoyl} PC (**3**, BH-C6PC), 1-fatty acyl-2-{8-[3-(4-hydroxyphenyl)-propionyl]-amino-octanoyl} PC (**4**, BH-C8PC), 1-fatty acyl-2-[12-[3-(4-hydroxyphenyl)-propionyl]-amino-dodecanoyl] PC (**5**, BH-C12PC), 1-fatty acyl-2-(12-{4-[3-(4-hydroxyphenyl)-propionyl]-aminobutanoyl}-aminododecanoyl) PC (**6**, BH-C16PC) and 1-fatty acyl-2-(12-{8-[3-(4-hydroxyphenyl)-propionyl]-amino-octanoyl}-aminododecanoyl) PC (**7**, BH-C20PC)

Each amino phospholipid (hydrochlorides of **23–28**) was reacted with BHR [23]. This coupling reaction was performed as follows. BHR (4.7 mg, 0.018 mmol) and triethylamine (4 μl , 0.031 mmol) were added with constant stirring to each amino phospholipid (**23–28**, approx. 0.015 mmol) dissolved in chloroform/methanol (5 : 1, v/v). After 2 h at 25 °C, the reaction was complete, as

revealed by TLC analysis. Solvents were evaporated under reduced pressure and each product (**2–7**) was purified by silica-gel column chromatography. Excess reagents were washed off first with solvent 3; subsequent elution with solvent 4 afforded pure products. Yields ranged between 60 % and 75 %. TLC analysis of each product in solvent 1 revealed a single slightly UV-positive spot, which stained with Molybdenum Blue but did not react with ninhydrin. **2**: TLC: R_f 0.24. $^1\text{H-NMR}$ [$\text{C}^2\text{HCl}_3/\text{C}^2\text{H}_3\text{O}^2\text{H}$, 10 : 1 (v/v), 300 MHz]: δ 0.67 (t, 3H), 1.10 (m, 24–28H), 1.37 (m, 2H), 1.49 (m, 2H), 1.98 (t, 2H), 2.12 (t, 2H), 2.23 (t, 2H), 2.63 (t, 2H), 2.93 (m, 2H), 2.98 (s, 9H), 3.36 (broad, 2H), 3.82 (m, 2H), 3.90–4.30 (broad and complex, 4H), 5.02 (m, 1H), 6.54 (d, 2H), 6.80 (d, 2H). **3**: TLC: R_f 0.25. $^1\text{H-NMR}$ (C^2HCl_3 , 300 MHz): δ 0.82 (t, 3H), 1.21 (m, 28–32H), 1.51 (m, 4H), 2.23 (overlapping triplets, 4H), 2.38 (t, 2H), 2.79 (t, 2H), 3.05 (m, 2H), 3.10 (s, 9H), 3.45 (broad, 2H), 3.95 (broad, 2H), 4.04–4.20 (broad and complex, 3H), 4.27 (dd, 1H), 5.15 (m, 1H), 6.69 (d, 2H), 6.96 (d, 2H). **4**: TLC: R_f 0.27. $^1\text{H-NMR}$ (C^2HCl_3 , 300 MHz): δ 0.82 (t, 3H), 1.20 (m, 32–36H), 1.51 (m, 4H), 2.22 (overlapping triplets, 4H), 2.35 (t, 2H), 2.78 (t, 2H), 3.05 (m, 2H), 3.10 (s, 9H), 3.48 (broad, 2H), 3.94 (broad, 2H), 4.02–4.20 (broad and complex, 3H), 4.28 (dd, 1H), 5.16 (m, 1H), 6.68 (d, 2H), 6.95 (d, 2H). **5**: TLC: R_f 0.29. $^1\text{H-NMR}$ (C^2HCl_3 , 300 MHz): δ 0.86 (t, 3H), 1.24 (m, 40–44H), 1.53 (m, 4H), 2.26 (overlapping triplets, 4H), 2.42 (t, 2H), 2.79 (t, 2H), 3.08 (m, 2H), 3.15 (s, 9H), 3.63 (broad, 2H), 3.87 (broad, 2H), 4.05–4.45 (broad and complex, 4H), 5.17 (m, 1H), 6.65 (d, 2H), 6.95 (d, 2H). **6**: TLC: R_f 0.30. $^1\text{H-NMR}$ (C^2HCl_3 , 300 MHz): δ 0.81 (t, 3H), 1.21 (m, 38–42H), 1.41 (m, 2H), 1.51 (m, 4H), 1.60 (m, 2H), 1.95 (t, 2H), 2.22 (overlapping triplets, 4H), 2.33 (t, 2H), 2.76 (t, 2H), 3.05 (m, 4H), 3.12 (s, 9H), 3.48 (broad, 2H), 3.91 (m, 2H), 4.08 (broad, 1H), 4.15 (broad, 2H), 4.31 (dd, 1H), 5.14 (m, 1H), 6.66 (d, 2H), 6.94 (d, 2H). **7**: TLC: R_f 0.32. $^1\text{H-NMR}$ (C^2HCl_3 , 300 MHz): δ 0.78 (t, 3H), 1.18 (m, 44–48H), 1.40 (m, 4H), 1.49 (m, 6H), 2.08 (t, 2H), 2.22 (overlapping triplets, 4H), 2.34 (t, 2H), 2.78 (t, 2H), 3.04 (m, 4H), 3.12 (s, 9H), 3.31 (broad, 2H), 3.92 (m, 2H), 4.05–4.30 (complex, 4H), 5.14 (m, 1H), 6.68 (d, 2H), 6.93 (d, 2H).

Radiolabelling of PCs derivatized with BHR (BHPCs)

Compounds **1–7** were radiolabelled with ^{125}I as follows. Each BHPC (70–100 μg , approx. 100 nmol), added from its stock solution in chloroform, was dried as a thin film in the bottom of a 5.6 mm \times 50 mm Pyrex glass tube under a stream of nitrogen. Buffer (100 μl , 20 mM sodium phosphates, pH 7.5) and three or four glass beads were then added. The tube was shaken vigorously for 1 min in a vortex-mixer and sonicated for 5 min at 25 °C. To this clear suspension, Na^{125}I (12 μl , 0.06 μCi), dissolved in 14 mM NaOH, and chloramine- τ (14 μg , 50 nmol) were added successively. After sonication of the mixture again for 30 s, the reaction proceeded for 15 min at 25 °C. Radioiodinated phospholipids were recovered in the organic phase after extraction with methanol (130 μl) and chloroform (150 μl). The products were purified by TLC on silica gel plates developed with solvent 1. In all cases, single spots were observed after autoradiography. After isolation, radioiodinated phospholipids (which co-migrated with unlabelled BHPCs) accounted for 30–40 % of the total radioactivity originally present in the reaction mixture.

Enzymic assays

A thin film of each phospholipid substrate was prepared as follows. A stock solution of each BHPC in chloroform (approx. 25 nmol, 10^5 c.p.m.) was evaporated under a stream of nitrogen in the bottom of a 5.6 mm \times 50 mm tube. Traces of organic

solvents were thoroughly eliminated by leaving the samples for 30 min under high vacuum. In the end, each phospholipid was solubilized (0.5 mM final concentration) in appropriate assay buffers [25 mM Hepes/1 mM CaCl_2 /16 mM Triton X-100 (pH 8.0) for the PLA_2 assay; 25 μM ZnCl_2 was added for the PLC assay], the samples were then heated to 100 °C for 40 s and finally sonicated at 30 °C for 5 min in a bath sonicator (Branson 2200; Branson Ultrasonics). After repetition of these last two steps, complete solubilization of the phospholipid substrates was verified by the quantitative recovery in the clear suspension of the radioactivity originally present in the sample. Enzymic reactions (50 μl final volume) were started by the addition of PLA_2 (170 ng) or PLC (19 ng) by the appropriate dilution of enzyme stock solutions (PLA_2 , 0.38 mg/ml in 50 mM borates buffer, pH 8.5; PLC, 0.5 mg/ml in 30 mM Tris/borates buffer, pH 7.1) in the corresponding assay buffers, together with BSA (1 mg/ml final concentration). Both phospholipase assays were run at 30 °C. The protein concentration of stock phospholipase solutions was determined by the method of Bradford [24]. Initial rates of hydrolysis were determined by removing 5 μl aliquots from each reaction mixture and adding 1 M HCl (10 μl) to stop the reaction. The latest time point was selected so that no more than 20% of the phospholipid substrate was hydrolysed. Under these conditions, a linear dependence of product yield was observed as regards time of reaction and enzyme concentration. After the reactions had been stopped, the samples were dried under high vacuum, dissolved in solvent 3 (15 μl) and loaded at 1 cm from the bottom of a 5 cm \times 5 cm TLC plate; this plate was developed with a two-solvent system: first with solvent 1 up to 2.5 cm and then, after the plate had been dried, with solvent 2 to the top. Under these conditions, BHPCs migrated with R_f values of approx. 0.27, BH-diacylglycerols with R_f approx. 0.63 and BH-fatty acids with R_f approx. 0.47. Indeed, a small trend exists in the chromatographic behaviour of these compounds: slightly higher R_f values were observed for the less polar compounds. Direct quantification of radioactivity present on the TLC plates was achieved by scraping the silica off the glass and counting the samples by scintillation.

Molecular modelling

Modelling of BHPCs within the binding cavity of PLA_2 was performed with MacroModel 5.5 and BatchMin 5.5 [25] installed on a Silicon Graphics O2 (R10000, 320 MB RAM, 4 GB hard disk) under the Irix 6.3 operating system. We used the MM2* force field (the version of Allinger's MM2 force field as implemented in MacroModel). MM2* force field uses distance-dependent dielectric electrostatics instead of the standard dipole-dipole electrostatics. All calculations were performed neglecting the ionization of the functional groups. The electrostatic interaction cut-off was set to 50 Å. For energy minimization we used a conjugate gradient method, with a final gradient of less than 0.05 $\text{kJ}\cdot\text{Å}^{-1}\cdot\text{mol}^{-1}$ (0.01 $\text{kcal}\cdot\text{Å}^{-1}\cdot\text{mol}^{-1}$) as the criterion for convergence.

RESULTS

Design and synthesis of new phospholipid substrates for phospholipases

A novel set of radioiodinatable PCs was synthesized to probe structural features of the phospholipid-binding cavity of phospholipases (Figure 1). These compounds differed in the length of the fatty acyl chain attached to the *sn*-2 position (from 3 to 25 atoms). With the exception of the shortest (BH-C0PC), this chain included at least one amide linkage. A common feature

of this family was the additional presence of a 4-hydroxyphenyl group at its end, which made these compounds suitable for radioiodination with chloramine-T. We expected that the choice of this range of lengths for the fatty acid bound to the *sn*-2 position would allow us to probe the effect of a bulky group equipped with a polar end at various distances along the path leading to the active site of phospholipases.

In BH-C0PC, the 4-hydroxyphenylpropionyl group (BH group) was bound directly to the glycerol moiety. Because of this, in this sole case, special protection of the hydroxy group as the acetyl ester was required to allow the acylation of the lysoPC moiety to proceed. In the end, selective deprotection of the phenol was achieved after reaction of Ac-BH-C0PC (compound **10**) with Zn in methanol (Scheme 1) [22]. For the following compounds of this series, BHR was used to acylate an ω -amino acid of various lengths attached to the *sn*-2 position (Scheme 2). Lastly, for the two longest PC substrates, an ω -amino acid four or eight carbon atoms in length was employed as an additional spacer arm between the BH group and the amino C12PC moiety (Scheme 3). Initially, attempts were made to build each modified fatty acid first, and then to acylate lysoPC with its corresponding anhydride. However, this seemingly straightforward procedure was unsuccessful. In the end, these BHPCs were synthesized starting from lysoPC by first acylating this compound with various N-tBOC-protected ω -amino acids and then growing the rest of this chain by stepwise deprotection and coupling reactions. This synthetic strategy proved to be the most efficient because (1) it required the smallest number of steps, (2) it minimized the steric hindrance at the critical acylation step by using in each case the shortest possible acyl anhydride, and (3) it facilitated the purification of all desired compounds along the synthesis, because all main products were PCs and were therefore readily isolatable from less polar by-products and excess reagents.

Enzymic assays of PLA_2 and PLC

All molecules assayed were substrates of PLA_2 and PLC (Figure 2). These compounds were presented to the enzymes in mixed micelles with Triton X-100. A phospholipid-to-detergent molar ratio of 1:32 proved to be effective in solubilizing all phospholipids assayed. Because no attempt was made to lower the proportion of detergent in the assay, this value should not be interpreted as the minimal ratio. However, the concentration of each enzyme in the assay was optimized so that the release of products exhibited a linear dependence with the time of hydrolysis up to 1 or 10 min, depending on the substrate being used (Figure 2A).

A similar pattern of activity for both PLA_2 and PLC assayed with these compounds was observed (Figure 2B): the three shortest BHPCs, namely BH-C0PC, BH-C4PC and BH-C6PC, were the poorest substrates; the activity increased as the *sn*-2 chain became longer, reaching an optimum for BH-C12PC and BH-C16PC, before decreasing with the longest substrate (BH-C20PC). When corrected for the surface dilution of each substrate in the micelle [26], the enzymic activity of BH-C12PC became comparable to that found for a PC with a fatty acyl chain of similar length [10,26] (result not shown). In addition, it is noteworthy that BH-C0PC, being the shortest molecule, was a significantly better substrate than the next compound in the series (BH-C4PC). Nevertheless, there were some important differences in the patterns of activity of the two enzymes: PLA_2 was considerably less efficient than PLC in hydrolysing the three shortest molecules, as attested by measuring the relative activity of each enzyme towards BH-C4PC in comparison with towards BH-C12PC: 0.35% and 9.5% for PLA_2 and PLC respectively.

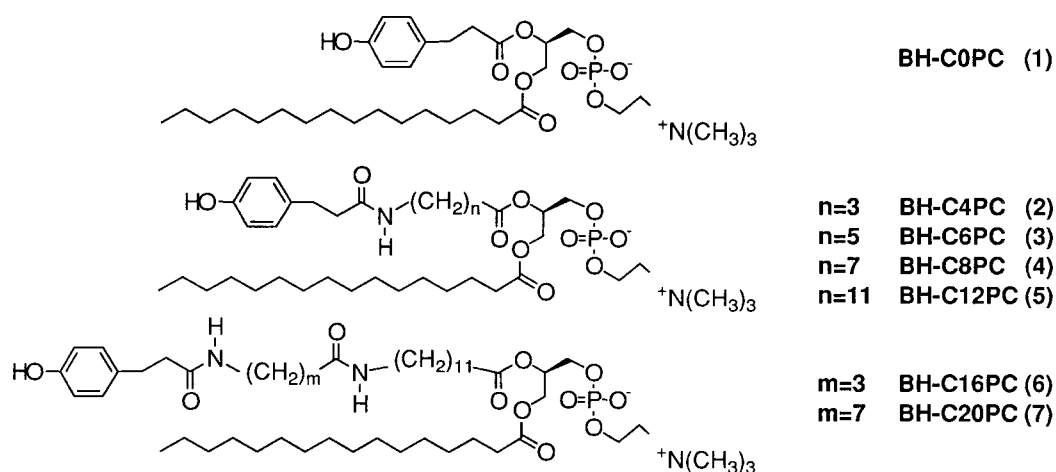
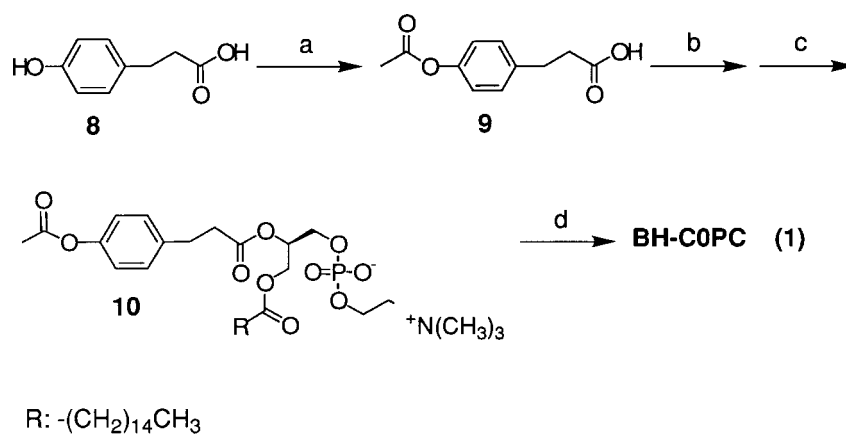
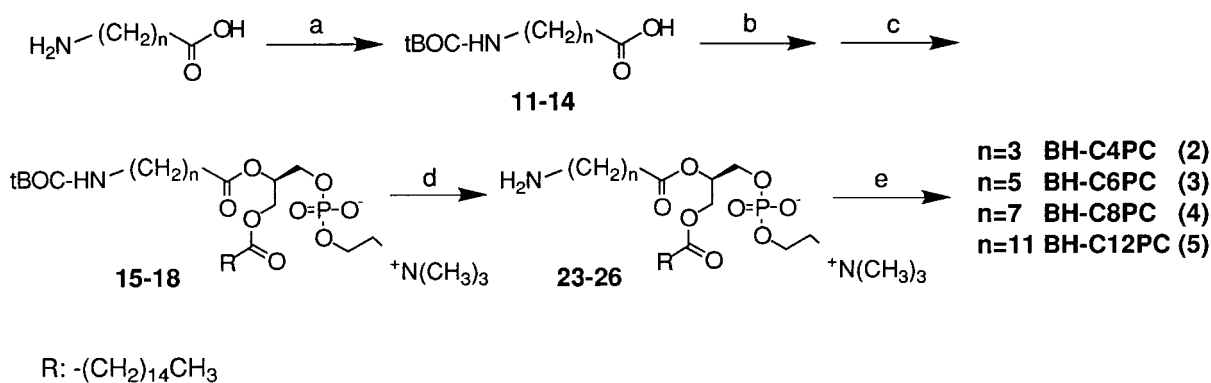


Figure 1 Set of radioiodinatable BHPCs



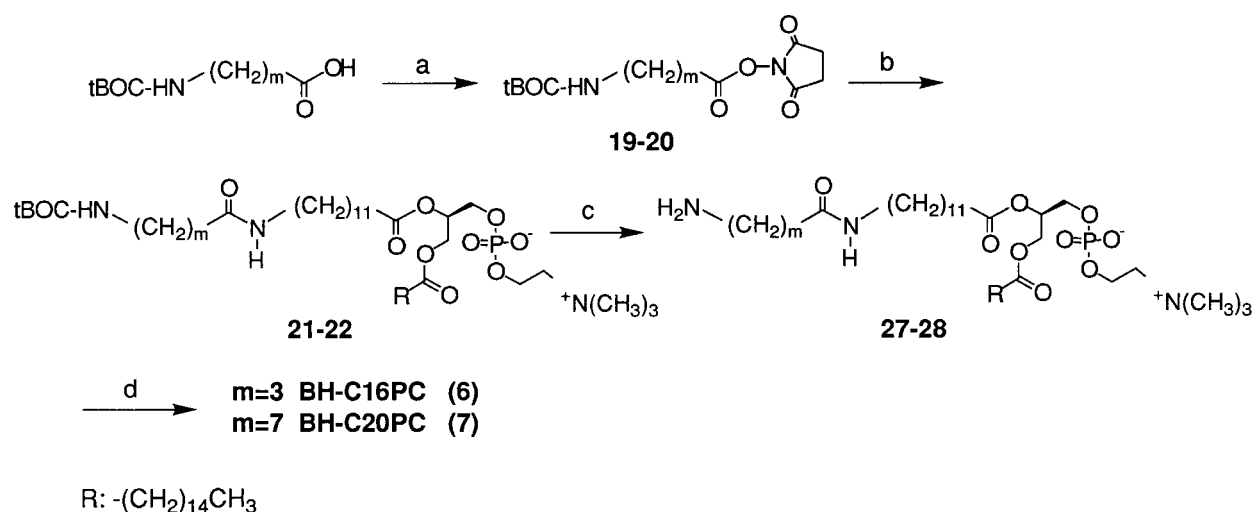
Scheme 1 Synthesis of BH-C0PC (1)

Reaction conditions were as follows: (a) acetic anhydride/HCl in chloroform; (b) DCC in anhydrous chloroform; (c) lysoPC and DMAP in anhydrous chloroform; (d) zinc dust in methanol.



Scheme 2 Synthesis of BH-C4PC (2), BH-C6PC (3), BH-C8PC (4) and BH-C12PC (5)

Reaction conditions were as follows: (a) di-*t*-butyl pyrocarbonate and DMAP in THF/aqueous NaOH; (b) DCC in anhydrous chloroform; (c) lysoPC and DMAP in anhydrous chloroform; (d) trifluoroacetic acid in chloroform with drops of methanol; (e) BHR and triethylamine in chloroform/methanol.



Scheme 3 Synthesis of BH-C16PC (6) and BH-C20PC (7)

Reaction conditions were as follows: (a) DCC and *N*-hydroxysuccinimide in anhydrous chloroform; (b) C12PC (**26**) in chloroform/methanol; (c) trifluoroacetic acid in chloroform with drops of methanol; (d) BHR and triethylamine in chloroform/methanol.

Similarly, the longest BHPC assayed (BH-C20PC) was a significantly worse substrate for PLA₂ than for PLC: 19% and 86% relative to BH-C12PC respectively.

Molecular modelling of BHPC-PLA₂ complexes

To evaluate the feasibility of the formation of complexes between different phospholipid substrates and PLA₂, we built molecular models employing MacroModel 5.5 [25]. For this purpose, the crystallographic structure of *N. naja atra* PLA₂ bound to a phosphonate transition-state analogue of phosphatidylethanolamine [14] [Brookhaven protein data bank (PDB) code 1POB] was used as the starting point.

For modelling the protein we proceeded as follows. Given the high degree of similarity between *N. naja atra* PLA₂ and *N. naja naja* PLA₂ (PDB code 1A3D), we replaced all six different amino acid side chains in the former with those found in the latter: i.e. Gln¹⁰ → Lys; Gly⁸¹ → Asp; Ala⁸⁸ → Ser; Asp¹⁰⁹ → Asn; Asn¹¹³ → Asp; an extra Gln residue was added to the C-terminus. Torsion angles along these side chains were preserved as in the original structure or inferred from a standard rotamer library where structural data were missing. Significantly, owing to their location, none of the amino acid residues in these positions (1) was predicted to compromise the overall tertiary structure of the protein or (2) interacted directly with the substrate analogue.

Next, a stepwise docking procedure of the BHPC substrates was achieved by sequential cycles of growth of each desired molecule inside the active site followed by local energy minimization. At the start of the model-building procedure of our substrates on this complex, we introduced the following modifications at the headgroup to mutate the analogue into a phospholipid. (1) The phosphonate group was replaced by a carbonyl group; the new oxygen atom occupied a position between those of the oxygen atoms in the parent phosphonate group. (2) The methylene group bound to the ether oxygen of the alkyl chain attached to position *sn*-1 was replaced by a carbonyl group. Similarly, the new oxygen atom was placed between the two former hydrogen atoms. (3) We decided to preserve the ethanolamine moiety instead of replacing it by choline, to prevent

an unnecessary steric clash at this positively charged centre. However, it is unlikely that any change at this end would have affected the conclusions drawn from the final models. (4) To generate a starting structure for the substrates, both fatty acyl chains were truncated to acetyl groups. It is noteworthy that none of these chemical modifications caused any unfavourable steric interaction with atoms belonging to either backbone or amino acid side chains of the protein. For the ensuing energy minimization steps, none of the atoms belonging to the above-described headgroup moiety was allowed to move.

From this point onwards, both fatty acyl chains were allowed to grow in a parallel fashion by the sequential addition of *trans* ethylene units. Similarly, the amide groups were added as *N*-methylacetamide units, also in their most stable *trans* conformation. Finally, the 4-hydroxyphenyl group was constructed in two steps: the phenylene group was positioned first and the hydroxy group was added later. During this growing procedure, energy minimization steps intervened to relax the tension present in intermediate structures. Free rotation was allowed around torsion angles along the fatty acyl chains.

A rigid framework including the amino acid residues comprising the walls of the binding cavity in PLA₂ was considered for fitting the growing ligand. This pocket consisted of a rigid substructure including all atoms within 6 Å of the substrate molecule. In the end, conformers of the substrates were found that corresponded to energy minima resulting from this spatially restrained calculation, as calculated *in vacuo* with the force field MM2* (Figure 3). In all cases, these complexes abode by the following criterion: that their energy be lower than that calculated after translation of the ligand out of the cavity, i.e. enzyme and substrate separated by approx. 100 Å. In no case was it necessary to translate the glycerol moiety additionally from the position seen in the crystallized analogue to make room for the hydrophobic portion of the substrate, i.e. the binding cavity always allowed enough space to fit both fatty acyl chains, even when the chain at position *sn*-2 included the bulky 4-hydroxyphenyl group in a position nearest to the polar headgroup (BH-C0PC). Moreover, a visual inspection of each model revealed that the ligand bound closely within the cavity. In agreement with this

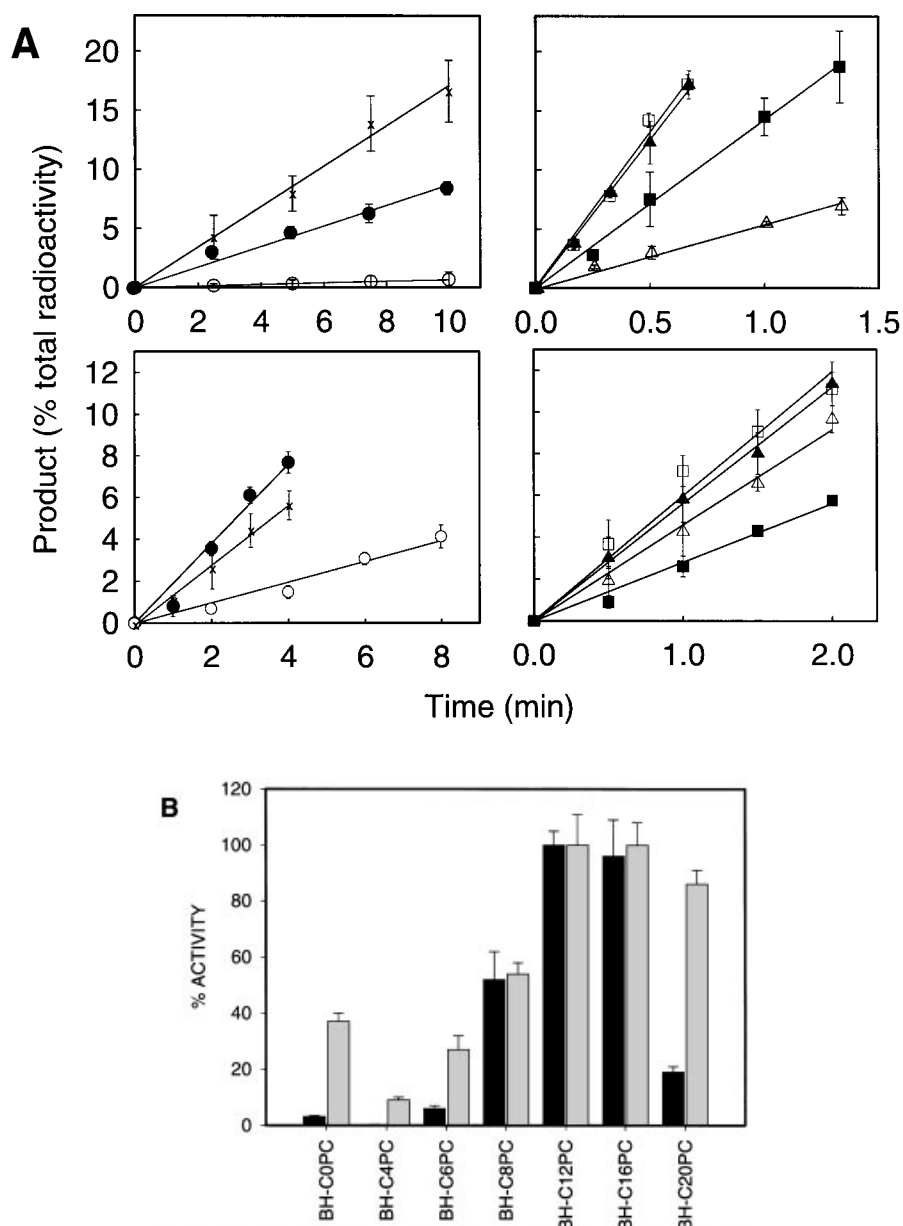


Figure 2 Hydrolysis of BHPCs by phospholipases

(A) Time course of hydrolysis of *N. naja naja* PLA₂ (upper panels) and *B. cereus* PLC (lower panels) assayed with ¹²⁵I-labelled BHPCs as substrates, in the presence of Triton X-100: ●, BH-C0PC; ○, BH-C4PC; ×, BH-C6PC; ■, BH-C8PC; □, BH-C12PC; ▲, BH-C16PC; △, BH-C20PC. The reaction conditions are reported in the Materials and methods section. Each experiment was run in duplicate. The ordinates are the percentage radioactivity associated with the products (fatty acid or diacylglycerol released after hydrolysis by PLA₂ or PLC respectively) relative to the total radioactivity present in each sample. Bars show S.E.M. (B) Relative rates of enzymic hydrolysis of ¹²⁵I-labelled BHPCs by *N. naja naja* PLA₂ (black bars) and *B. cereus* PLC (grey bars) assayed in the presence of Triton X-100. Under conditions appropriate for measuring the initial velocity, the enzymic activity (height of each bar) was derived from the slope of the graph representing the time course of phospholipid hydrolysis (A), as estimated by linear regression analysis. The S.E.M. of the slope is shown on each bar. Rates of hydrolysis are expressed as percentages of that for the substrate that showed the greatest activity (BH-C12PC, 5). Under the experimental conditions chosen for these assays (0.5 mM substrate, 16 mM Triton X-100, 25 mM Hepes buffer, pH 8.0, 1 mM CaCl₂ and 3.4 μg/ml for PLA₂, or 25 μM ZnCl₂ and 0.38 μg/ml for PLC; 30 °C), the absolute rates of hydrolysis of BH-C12PC with PLA₂ and PLC were 40 ± 2 and 74 ± 8 μmol of phospholipid/min per mg of protein respectively.

observation, there was no significant spatial overlap between atoms of any of the phospholipid analogues and the amino acid side chains lining the walls of the cavity, i.e. in all cases the overlapping volume was less than 3% of the total van der Waals volume of the ligand (results not shown). This extensive close contact of the hydrophobic moieties of the ligand within its binding site is indeed observed for the crystallized complex of

PLA₂ with the transition-state analogue, where both chains are aliphatic [14]. A similar circumstance occurred in our models, in which the BH group became embedded into the binding pocket. This apparent paradox is explained by recognizing the fact that the binding site resembles more a deep and open cleft than a narrow channel leading to the catalytic site. This feature permits lateral movement of the fatty acyl chain at position *sn*-1, thus

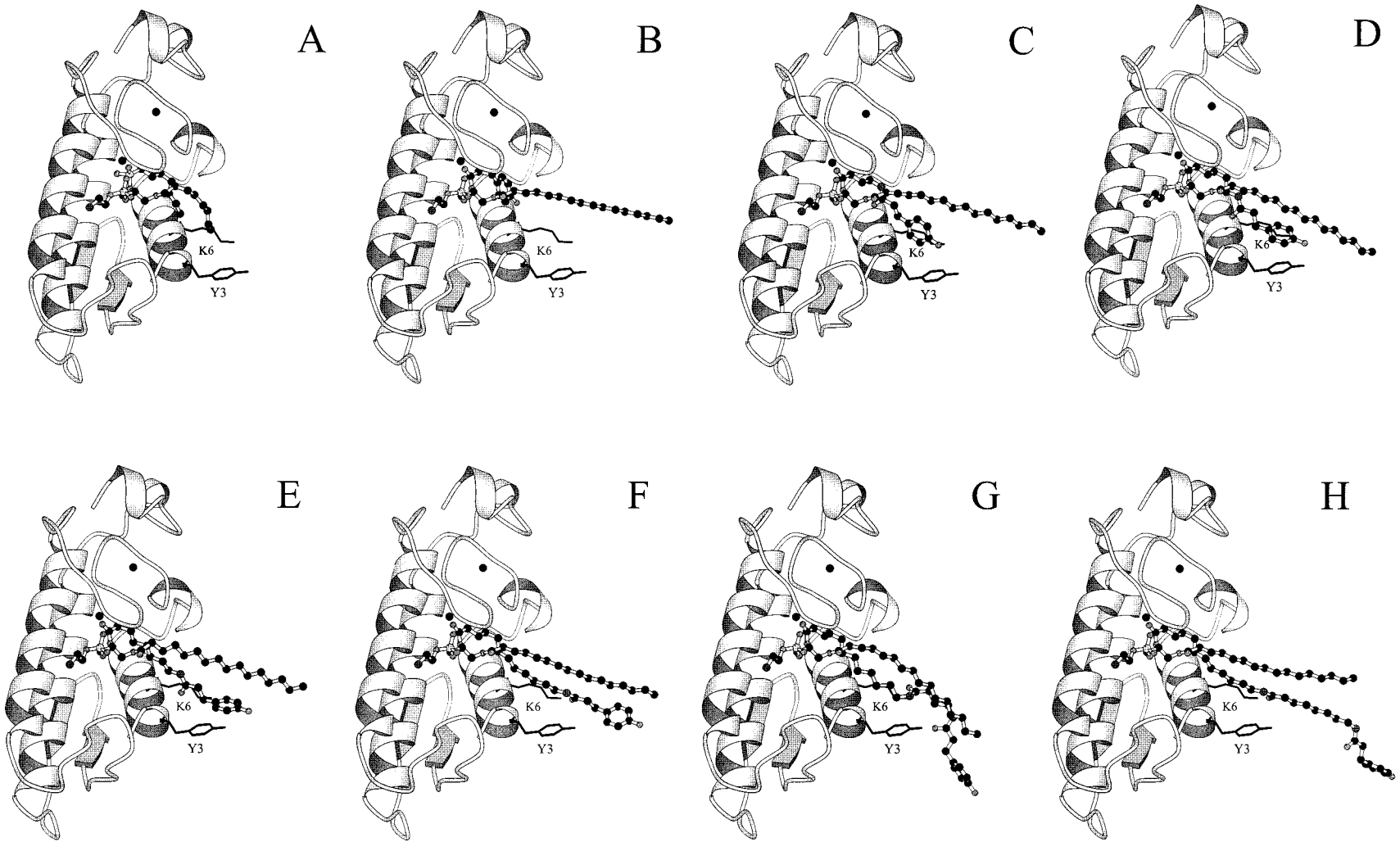


Figure 3 Schematic view of BHPCs bound to PLA₂

(A) Ribbon representation of PLA₂ from *N. naja atra* bound to a ball-and-stick model of a transition-state analogue of phosphatidylethanolamine, as determined by X-ray crystallographic analysis [14] (PDB code 1POB). Black circles indicate the positions of bound Ca²⁺ ions. Relevant amino acid side chains mentioned in the text (Tyr³ and Lys⁶) are also shown. Ball-and-stick models of BH-C0PC (B), BH-C4PC (C), BH-C6PC (D), BH-C8PC (E), BH-C12PC (F), BH-C16PC (G) and BH-C20PC (H) bound to *N. naja naja* PLA₂ are shown side by side. These images were generated with the program MolScript [38], version 1.4.

Table 1 Location of relevant functional groups along the *sn*-2 fatty acyl chain relative to the protein surface in BHPC-PLA₂ complexes

In the models shown in Figure 6, distances were measured between selected atoms along the *sn*-2 acyl chain in the phospholipid substrate and atoms belonging to amino acid residues located at the edge of the binding pocket, on the surface of *Naja naja naja* PLA₂. A minus sign indicates a location inside or tangential to the protein surface, conversely, a positive distance denotes a position outside the protein. Phenyl_{BH}-phenyl_{Tyr3} distances were measured from the centre of mass of the phenyl ring of the BH moiety to the centre of mass of the phenyl ring of Tyr³. CO_{amide}-N_{εK6} distances were measured from the amide carbonyl oxygen most proximal to the glycerol backbone to the ε-amino nitrogen of Lys⁶. For BH-C0PC, the ester carbonyl oxygen was considered instead.

Substrate	Distance (Å)	
	Phenyl _{BH} -phenyl _{Tyr3}	CO _{amide} -N _{εK6}
BH-C0PC	-11.4	-16.4
BH-C4PC	-5.4	-9.7
BH-C6PC	-3.7	-7.9
BH-C8PC	+4.4	-4.9
BH-C12PC	+7.6	-2.3*
BH-C16PC	+8.7	-2.2*
BH-C20PC	+16.3	-2.1*

* These distances lie well within the acceptable limit (less than 2.5 Å) for a canonical hydrogen bond.

allowing enough space to accommodate a bulkier and more rigid aromatic group. Overall, the conformation of fatty acyl chains predicted for the BHPC substrates bound to PLA₂ was similar to that generally accepted to occur in aggregates of PCs found in crystals or membranes [27]. Thus it was expected that no major structural distortion of this moiety should be required for catalysis to take place.

For this series of substrates, the occurrence of specific interactions between the modified fatty acyl chain and protein atoms was analysed as a function of the position of the BH moiety along the substrate-binding channel. More specifically, the depth at which the BH group lay within the protein was evaluated by measuring the distance from the centre of mass of the phenyl ring of BH to the centre of mass of the phenyl ring of Tyr³, a residue located on the surface of the protein and in a position adjacent to the path of the *sn*-2 chain (Table 1). For the three shortest compounds (BH-C0PC, BH-C4PC and BH-C6PC; Figures 3B-3D) the 4-hydroxyphenyl group lay inside the hydrophobic pocket of the enzyme, whereas for BH-C8PC (Figure 3E) this group protruded just above the protein surface. In contrast, the three longest substrates (BH-C12PC, BH-C16PC and BH-C20PC; Figures 3F-3H) placed the 4-hydroxyphenyl ring outside the enzyme. The snug fit observed for the first four substrates between the fatty acyl chains and atoms lining the walls of the cavity could give rise to specific interactions. Here, aromatic-aromatic stacking [28] and amino-aromatic interactions [29] could involve the BH ring, which, as the *sn*-2 chain grew, progressively came into close contact with the side chains of the following residues: Phe⁵, Lys⁶, Leu², Tyr³ and Trp¹⁸. In no case did the hydroxy group of the BH group hydrogen-bond with the backbone or side chains atoms of the protein, pointing to the hydrophobic nature of this patch of protein surface. Similarly, for those substrates endowed with amide groups on their *sn*-2 fatty acyl chain, no chance for hydrogen bond formation was predicted as long as this functional group was located within the cavity (as occurred with BH-C4PC, BH-C6PC and BH-C8PC). In addition, the search for possible hydrogen-bond partners along the binding site was completed by allowing free rotation

around the C-NHCO bond, yielding neither a suitable acceptor for the NH group nor a donor for the CO group. When the amide group reaches the surface of the protein (as occurred with BH-C12PC, BH-C16PC and BH-C20PC), a hydrogen bond was formed between the carbonyl oxygen atom of the amide in position 12 of the *sn*-2 chain and the amino group of Lys⁶ (Table 1). A similar analysis performed for the hydroxy group of BH indicated that in no case did this group hydrogen-bond with atoms belonging to the binding cavity.

Although the structure of PLC is also known at atomic resolution [16] (PDB code 1AH7), a similar model-building analysis of substrates complexed to this enzyme was hampered by the lack of a detailed picture of the binding mode of phospholipids to the active site. Even though a crystal structure was reported for PLC from *B. cereus* complexed with a substrate analogue (phosphorylcholine) [30], only the atomic coordinates for the enzyme (no substrate analogue) are currently available in PDB.

DISCUSSION

Design and synthesis of BHPCs

A novel series of PCs were synthesized (Figure 1) to investigate structural aspects of substrate recognition by PLA₂ and PLC. A variable-length fatty acyl chain attached to position *sn*-2 is capped with the bulky and polar 4-hydroxyphenyl group. Except for BH-C0PC, one or two amide linkages intervene along this chain. A common feature of members of this series is the presence of a saturated fatty acyl chain 16 (or 18) carbon atoms long at position *sn*-1. The use of these substrates allowed us to survey the substrate entrance channel in phospholipases with a sizeable polar probe. In addition, the amide linkages permitted the examination of possible hydrogen-bonding within this channel. To achieve this goal, the chain length had to span a wide range (3-25 atoms), enough to locate the end group inside or outside the enzyme, once the phospholipid head group had become adequately docked for catalysis.

The use of one radioiodinated phospholipid analogue of this kind was advanced in an early study to examine vesicle-vesicle and vesicle-cell transfer [31]. Although this compound was indeed a substrate of phospholipases, the focus of that study was its use as molecular marker for metabolic studies. The synthetic approach involved the classical use of BHR, whereby this reagent was first radioiodinated and the target molecule bearing the amino group was next chemically modified. In contrast with this, our approach renders all phospholipids as non-radioactive precursors suitable for radioiodination at the very last stage, following a usual oxidative protocol. An additional practical advantage is the fact that our BHPCs can serve as starting materials for obtaining a variety of other radioiodinatable lipids of biological interest (diacylglycerol, phosphatidic acid or fatty acids).

Mixed detergent/phospholipid system for the enzymic assay of phospholipases

It is well known that phospholipase activity depends strongly on the aggregation state of the substrate [8,32]. Because the series of BHPCs synthesized here span a wide range of lengths of the fatty acyl chain at position *sn*-2, their physicochemical properties will vary accordingly. Indeed, a subtle variation in the mobility of these compounds as analysed by TLC (maximal difference in R_f , approx. 0.08) was observed, correlating well with chain length and the number of amide linkages. Therefore, and to standardize the aggregation state of the substrate offered to the enzymes,

each BHPC was dispersed with a large excess of Triton X-100 (1:32, on a molar basis) to yield mixed-micelle populations [26].

The rate-limiting step for phospholipase catalysis in micellar systems could be the mass transfer of enzyme and/or substrate molecules between micelles rather than the intrinsic interaction of the substrate with the enzyme [33]. However, another line of evidence indicated that this does not seem to be true of the Triton X-100/PC mixed-micelle system [34]. Results given in the present paper support the view that mass transfer processes do not control the overall catalytic rate measured. Otherwise, one would expect significantly higher enzymic activity for the shortest substrates (BH-C0PC, BH-C4PC and BH-C6PC) because of their predictably high critical micelle concentrations and hence their faster exchange rates. On the contrary, we found that these molecules are the worst substrates of this series. In contrast, the expectation holds that all members of this series of phospholipids will exchange more readily between micelles or vesicles than typical phospholipids, owing to the presence of heteroatoms and/or aromatic substituents in the *sn*-2 fatty acyl chain [31,34].

Structure of BHPCs influences the hydrolytic activity of phospholipases

The enzymic activity profile of phospholipases towards BHPCs depends strongly on specific structural characteristics of the fatty acyl chain attached to position *sn*-2. Further insight into this recognition process was revealed by modelling the binding mode of each substrate to PLA₂. Qualitatively, the behaviour of phospholipases towards BHPCs obeys the general trend classically observed for aliphatic PCs of various lengths: the enzymic activity increases as the fatty acyl chain grows to an optimal length, beyond which the activity falls [10]. Nevertheless, two important differences should be pointed out: (1) the range of enzymic activities measured for BHPCs, i.e. the ratio of BH-C12PC to BH-C4PC is approx. 290 for PLA₂ and approx. 11 for PLC, extends well beyond that observed for aliphatic PCs, and (2) the optimal length for the fatty acyl chain at *sn*-2 in BHPCs is 16 atoms (BH-C12PC), whereas dioctanoyl PC (or diheptanoyl PC for PLC) [9,10] is the best substrate in the aliphatic series.

Models of BH-C0PC, BH-C4PC and BH-C6PC docked to PLA₂ show that the phenyl ring is confined at different depths inside the binding cavity (Figures 3B–3D). The mere presence of a bulky, rigid and polar aromatic group instead of an aliphatic chain will most probably interfere with optimal substrate recognition. These constraints will disappear as the chain length reaches (or exceeds) 11 atoms (BH-C8PC, Figure 3E), in agreement with results from enzymic activity (Figure 2B). In connection with this, a previous study with methyl-branched fatty acyl PCs showed that steric hindrance negatively affects catalysis only when both fatty acyl chains are modified [35]. This effect fades sharply as the branching point advances between one and four carbon atoms towards the end of the chain. However, an explanation for these results does not exclude the possibility of an inappropriate orientation of the substrate, which would interfere with catalysis. At variance with this study, in the BHPC series, the 4-hydroxyphenyl group tethered to the fatty acyl chain at *sn*-2 allowed us to probe steric hindrance at positions far removed from the catalytic site, thus defining the optimal chain length for the complete entry of a linear moiety into the substrate channel. In this regard, BH-C8PC complies with this requirement (Figure 3E and Table 1). Nevertheless, additional variables have to be taken into consideration for a full explanation of the results observed (Figure 2B).

Inspection of the surface of the substrate channel in PLA₂ reveals few, if any, polar groups available for hydrogen-bonding.

This feature influences the interaction of BHPCs with the enzyme, owing to the presence of the terminal hydroxy group and/or the linking amide in the substrate. Indeed, the existence of unsatisfied hydrogen-bond donor or acceptor groups within this hydrophobic milieu (as occurs with BH-C0PC, BH-C4PC, BH-C6PC and BH-C8PC) hampers catalytic efficiency, presumably owing to decreased binding energy. This is a recognized phenomenon affecting the strength and specificity of interaction at protein–protein interfaces (reviewed in [36]). In contrast, the three longest substrates (BH-C12PC, BH-C16PC and BH-C20PC) are predicted to form a hydrogen bond with the ϵ -amino group of Lys⁶, a residue placed at the edge of the entry to the cavity. Alternatively, the amide group of these substrates could hydrogen-bond to solvent molecules, thus obliterating any unfavourable energetic contribution to binding. In contrast, the use of micellized substrates minimizes the exposure to the aqueous milieu of the hydrophobic portions of the tail projecting outside the binding cavity. Taking all these elements into consideration, we conclude that BH-C12PC and BH-C16PC best avoid these adverse energetic contributions, thus explaining their behaviour as optimal substrates.

The extreme compounds in this series, namely BH-C0PC and BH-C20PC, exhibit anomalous behaviour, a point that merits further analysis. BH-C0PC is a significantly better substrate for both PLA₂ and PLC than its immediate neighbour BH-C4PC. From the model of BH-C0PC docked to PLA₂ (Figure 3B), it becomes evident that the absence of an amide linkage in this compound circumvents any negative energetic effect arising from the failure to establish a hydrogen-bond network, as is presumably also true of BH-C4PC. In addition, the shape of BH-C0PC resemble more an inverted cone than a typical cylinder [27]. In this regard, phospholipase activity might also be positively influenced by this factor, because extraction of this substrate from the micellar support is facilitated. In contrast, BH-C20PC shows a substantially decreased efficiency as a substrate for PLA₂. An increased activation energy barrier for the extraction step of this lipid from the micelle is expected owing to its excessive chain length. Besides, a conformation might exist in which the fatty acyl chain at *sn*-2 loops back, so that the terminal hydroxy group resurfaces into the aqueous milieu. In any of these models, an impairment of optimal catalytic efficiency will result. In this context, it is known that a constraint on the vertical movement of the substrate negatively affects the activity of phospholipases [12,37].

In contrast, PLC behaves as a less discriminating enzyme than PLA₂ towards this series of substrates (Figure 2B), as has been extensively documented for other PCs [9–11]. However, the magnitude of the differences in catalytic efficiency seen for BHPCs are among the largest ever reported, a likely consequence of the major structural modifications introduced here. The catalytic site of *B. cereus* PLC is located at the end of a hydrophobic channel, as shown by crystallographic and structure–activity studies [16]. In this case, the same considerations of substrate structure should be invoked to explain the common general trend observed. Nevertheless, the putative entrance channel for the substrate in PLC is broader and shallower than that in PLA₂, bringing about a less pronounced activity pattern for the former enzyme. Constraints on the vertical movement of the substrate are less stringent in PLC [12,37], as documented here by the behaviour of BH-C20PC, for which the increased chain length caused only a minor detrimental effect on enzymic activity.

The good agreement found between the pattern of enzymic activity with different substrates and the predictions from molecular models based on a crystallographic structure supports the

validity of the latter as a reliable representation of the enzyme working at the water/lipid interface. The choice of phospholipid substrates of various lengths tethered to functional groups proved to be a useful tool for probing the topography of the binding cavity in phospholipases; its usefulness can be extended to study other lipid-protein interactions. This work highlights the value of a combined approach blending experimental and computational results to unravel structural features of an enzyme-substrate recognition phenomenon.

We dedicate this work to Professor Alejandro C. Paladini on the occasion of his 80th birthday. We thank Ms. Cecilia N. Arighi for her advice on the use of molecular modelling software. This work was supported by grants (to J.F.C. and J.M.D.) from the National Research Council of Argentina (CONICET), the University of Buenos Aires (UBACYT), Fundación Antorchas and the European Union. J.J.C. is the recipient of a graduate student fellowship from the University of Buenos Aires.

REFERENCES

- Dennis, E. A., Rhee, S. G., Billah, M. M. and Hannun, Y. A. (1991) *FASEB J.* **5**, 2068–2077
- Exton, J. H. (1994) *Biochim. Biophys. Acta* **1212**, 26–42
- Liscovitch, M. and Cantley, L. C. (1994) *Cell* **77**, 329–334
- Moolenaar, W. H. (1995) *J. Biol. Chem.* **270**, 12949–12952
- Nishizuka, Y. (1992) *Science* **258**, 607–614
- Spiegel, S., Foster, D. and Kolesnick, R. (1996) *Curr. Opin. Cell Biol.* **8**, 159–167
- Gijon, M. A. and Leslie, C. C. (1999) *J. Leukoc. Biol.* **65**, 330–336
- Wells, M. A. (1974) *Biochemistry* **13**, 2248–2257
- El-Sayed, M. Y., DeBose, C. D., Coury, L. A. and Roberts, M. F. (1985) *Biochim. Biophys. Acta* **837**, 325–335
- Roberts, M. F., Otnaess, A.-B., Kensil, C. A. and Dennis, E. A. (1978) *J. Biol. Chem.* **253**, 1252–1257
- Lewis, K. A., Bian, J., Sweeney, A. and Roberts, M. F. (1990) *Biochemistry* **29**, 9962–9970
- Soltys, C. E., Bian, J. and Roberts, M. F. (1993) *Biochemistry* **32**, 9545–9552
- Delfino, J. M., Florin-Christensen, J., Florin-Christensen, M. and Richards, F. M. (1994) *Biochem. Biophys. Res. Commun.* **205**, 113–119
- White, S. P., Scott, D. L., Otwinowski, Z., Gelb, M. H. and Sigler, P. B. (1990) *Science* **250**, 1560–1563
- Scott, D. L., Otwinowski, Z., Gelb, M. H. and Sigler, P. B. (1990) *Science* **250**, 1563–1566
- Hough, E., Hansen, L. K., Birknes, B., Jynge, K., Hansen, S., Hordvik, A., Little, C., Dodson, E. and Derewenda, Z. (1989) *Nature (London)* **338**, 357–360
- Hansen, S., Hough, E., Svensson, L. A., Wong, Y.-L. and Martin, S. F. (1993) *J. Mol. Biol.* **234**, 179–187
- Scott, D. L., White, S. P., Otwinowski, Z., Yuan, W., Gelb, M. H. and Sigler, P. B. (1990) *Science* **250**, 1541–1546
- Waggoner, A. S. and Stryer, L. (1970) *Proc. Natl. Acad. Sci. U.S.A.* **67**, 579–589
- Hubbell, W. L. and McConnell, H. M. (1971) *J. Am. Chem. Soc.* **93**, 314–326
- Gupta, C. M., Radhakrishnan, R. and Khorana, H. G. (1977) *Proc. Natl. Acad. Sci. U.S.A.* **74**, 4315–4319
- González, A. G., Jorge, Z. D., López Dorta, H. and Rodríguez Luis, F. (1981) *Tetrahedron Lett.* **22**, 335–336
- Bolton, A. E. and Hunter, W. M. (1973) *Biochem. J.* **133**, 529–539
- Bradford, M. M. (1976) *Anal. Biochem.* **72**, 248–254
- Mohamadi, F., Richards, N. G. J., Guida, W. C., Liskamp, R., Lipton, M., Caufield, C., Chang, G., Hendrickson, T. and Still, W. C. (1990) *J. Comput. Chem.* **11**, 440–467
- Dennis, E. A. (1973) *Arch. Biochem. Biophys.* **158**, 485–493
- Gennis, R. B. (1989) in *Biomembranes* (Cantor, C. R., ed.), pp. 36–40 and 55–65, Springer Verlag, New York
- Burley, S. K. and Petsko, G. A. (1985) *Science* **229**, 23–28
- Burley, S. K. and Petsko, G. A. (1986) *FEBS Lett.* **203**, 139–143
- Hansen, S., Hough, E., Svensson, L. A., Wong, Y.-L. and Martin, S. F. (1993) *J. Mol. Biol.* **234**, 179–187
- Schroitt, A. J. and Madsen, J. W. (1983) *Biochemistry* **22**, 3617–3623
- Deems, R. A., Eaton, B. R. and Dennis, E. A. (1975) *J. Biol. Chem.* **250**, 9013–9020
- Jain, M. K., Rogers, J., Hendrickson, H. S. and Berg, O. G. (1993) *Biochemistry* **32**, 8360–8367
- Soltys, C. E. and Roberts, M. F. (1994) *Biochemistry* **33**, 11608–11617
- DeBose, C. D., Burns, Jr, R. A., Donovan, J. M. and Roberts, M. F. (1985) *Biochemistry* **24**, 1298–1306
- Janin, J. and Chothia, C. (1990) *J. Biol. Chem.* **265**, 16027–16030
- Lewis, K. A., Soltys, C. E., Yu, K. and Roberts, M. F. (1994) *Biochemistry* **33**, 5000–5010
- Kraulis, P. J. (1991) *J. Appl. Crystallogr.* **24**, 946–950

Received 21 September 1999/16 November 1999; accepted 23 December 1999